Exchange bias of polycrystalline antiferromagnets with perfectly compensated interfaces

D. Suess,* M. Kirschner, T. Schrefl, and J. Fidler
Institute of Solid State Physics, Vienna University of Technology, Wiedner Hauptstrasse 8-10, A-1040 Vienna, Austria

R. L. Stamps and J.-V. Kim
School of Physics, University of Western Australia, 35 Stirling Highway, Crawley WA 6009, Australia
(Received 7 October 2002; published 28 February 2003)

A mechanism for exchange bias and training for antiferromagnet/ferromagnet bilayers with fully compensated interfaces is proposed. In this model, the bias shift and coercivity are controlled by domain-wall formation between exchange-coupled grains in the antiferromagnet. A finite element micromagnetic calculation is used to show that a weak exchange interaction between randomly oriented antiferromagnetic grains and spin-flop coupling at a perfectly compensated interface are sufficient to create shifted hysteresis loops characteristic of exchange bias. Unlike previous partial wall models, the energy associated with the unidirectional anisotropy is stored in lateral domain walls located between antiferromagnetic grains. We also show that the mechanism leads naturally to a training effect during magnetization loop cycling.

DOI: 10.1103/PhysRevB.67.054419 PACS number(s): 75.50.Ee, 75.40.Mg, 75.60.Jk, 75.70.Kw

I. INTRODUCTION

The story of exchange bias began more than forty years ago.[1] Most recently, possible device applications have renewed interest in exchange bias and highlighted the need for a quantitative understanding of the phenomenon. Some of the more commonly studied materials use sputtered IrMn and MnFe antiferromagnetic films.[2] A successful model for exchange bias should therefore be able to describe loop shifts and coercivity for polycrystalline films. Additionally, the theory should also be able to describe effects of well-defined interfaces between the ferromagnet and antiferromagnet such as what one might expect for systems using CoO (Ref. 3) or NiO.[4] A particular challenge is to explain exchange bias in the case of perfectly compensated interfaces,[5,6] and also to understand the sometimes observed insensitivity of measured bias to supposed interface structures.[7]

The realization that many complex processes can be involved was first put forward by Néel in attempts to understand coercivity and training effects.[8] In a more recent model the intergranular coupling between antiferromagnet (AF) grains account for the training effect.[9] Additional developments were made by Malozemoff *et al.* when explaining the possibility of effects due to domain-wall pinning, partial wall formation in the antiferromagnet, and spin-order reconstruction at the interface of the antiferromagnet and ferromagnet.[10,11,5] Two of the most recent suggestions for bias mechanisms concentrate on the role of domain pinning by defects in semirandom antiferromagnets,[14] and the formation of lateral walls between steps at uncompensated interfaces.[12]

A key element of all later developments has been the recognition of magnetization processes in the antiferromagnet on measurable features associated with the bias. Typically, the problem has been to understand exchange bias in the presence of imperfections and defects.

In this paper we suggest a mechanism by which energy can be stored in the antiferromagnet, which relies on random distributions of grains. Most importantly, we show that a system with perfectly compensated interfaces, free of defects and other structural imperfections within grains, can still exhibit exchange bias. This is in contrast to previous theories[13] that require some sorts of imperfections, either at the interface or within the antiferromagnet, in order to produce exchange bias in a mostly compensated interface structure.

Consider a ferromagnetic film exchange coupled to an ensemble of antiferromagnetic grains. Even if the interface is assumed to be everywhere perfectly compensated, spin-flop canting at the interface can provide a small net magnetic moment to which the ferromagnet can couple. The spin-flop configuration is not stable without certain effective anisotropies, and will not lead to exchange bias for realistic antiferromagnet material parameters. The reason is that during magnetization reversal, a canted antiferromagnetic interface is unstable to out-of-plane fluctuations and can nucleate a reversal of the antiferromagnet sublattices.[6] This can result in coercivity, but does not produce a shifted hysteresis loop for the ferromagnet.

An interesting possibility appears if the uniaxial anisotropy axes of the individual antiferromagnetic grains are randomly oriented. The significance of a distribution of uniaxial directions lies in the different effects which reversal of the ferromagnet produces for different axis orientations. To appreciate this, consider how a canted antiferromagnetic grain exchange coupled to a single domain ferromagnetic grain reverses with the ferromagnet. The spin-flop configuration expected for a compensated interface can be represented schematically as shown in Fig. 1. The thick arrow represents the ferromagnet spins, and the arrows labeled **a** and **b** are the two antiferromagnet sublattices. A spin-flop configuration is shown in Fig. 1(a) where the dotted line is the orientation of the antiferromagnet uniaxial axis. The anisotropy energy involved in the spin-flop configuration is given by $E_{\mathrm{ani}} = -K_1(a_z^2+b_z^2)/M^2$, where K_1 is the anisotropy energy and M is the sublattice magnetization. a_z and b_z are the projection of the magnetization of sublattices A and B on the easy axis, respectively.

Suppose now that the interlayer exchange coupling is

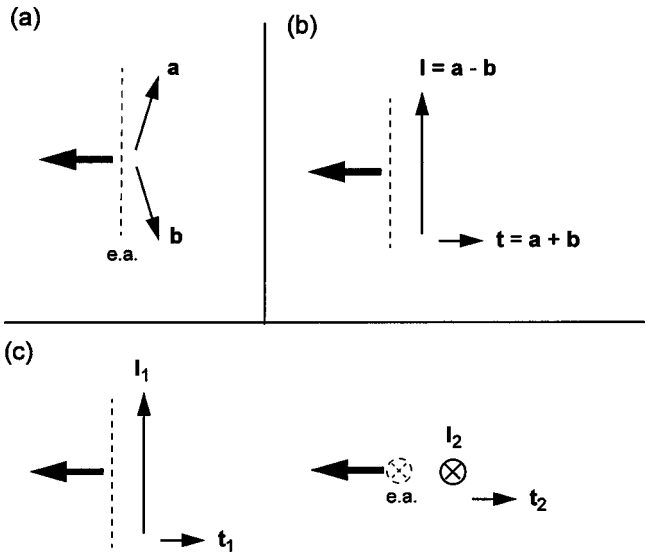

FIG. 1. (a) Spin structure at a compensated interface between a ferromagnet and antiferromagnet. The thick arrow denotes the magnetization in the ferromagnet. The arrows **a** and **b** represent the magnetizations of sublattice *A* and sublattice *B* in the antiferromagnet, respectively. The dotted line is the easy axis direction in the antiferromagnet. (b) The same spin structure described with a different notation. (c) The left and right images show spin configurations in the antiferromagnet for an anisotropy direction in the antiferromagnet parallel to the image plane and perpendicular to the image plans, respectively.

comparable in magnitude to the antiferromagnetic exchange and anisotropies such that the spin-flop configuration can rotate rigidly when a field is applied. Reversal of the ferromagnet under application of a small applied field will cause both sublattice spins to rotate with the ferromagnet. Rotations about the anisotropy axis of the antiferromagnet leave E_{ani} unchanged and are reversible. Rotations about any other direction change E_{ani} and can involve irreversible changes in the magnetic configuration. Reversal of the ferromagnet and spin-flop antiferromagnet with a random distribution of antiferromagnet uniaxial anisotropy axes therefore involves both reversible and irreversible changes in the antiferromagnet.

If the antiferromagnet grains do not interact via exchange coupling across intergrain boundaries, coercivity will be observed in the antiferromagnet in proportion to the fraction of irreversibly switched grains, but there will not be a shifted hysteresis. The shifted hysteresis will appear only if the energy of the system changes upon reversal. This can occur in the random axis spin-flop model described above if interactions between antiferromagnet grains exist. The reason can be seen using the notation defined in Fig. 1(b). The vector **l** is the projected sum of the sublattice magnetizations on the anisotropy axis of a grain, and the vector **t** is the component of the sublattice magnetization sum perpendicular to the anisotropy axis.

Suppose two grains have antiferromagnet anisotropy axes aligned as shown in Fig. 1(c) with the only difference that the angle between the easy axes in the two grains is not exactly 90°. Consider what happens if the ferromagnet reverses by rotating around $\mathbf{l}_1$. The angle between $\mathbf{l}_1$ and $\mathbf{l}_2$ will change during reversal since the angle between $\mathbf{l}_1$ and $\mathbf{l}_2$ is not zero or 90°. The change in angle will involve a change in intergranular exchange energy. This means that the magnitude of the intergranular exchange energy can change upon reversal of the ferromagnet, depending on the relative orientation of anisotropy axes for adjacent grains.

During reversal in a planar geometry where the ferromagnet is constrained by demagnetizing fields to lie in the film plane, the spins in antiferromagnetic grains with axes nearly perpendicular to the interface will not be strongly affected by the changing orientation of the ferromagnet. This is in contrast to the spins in antiferromagnetic grains with axes parallel to the interface, in which it is not possible for the spin-flop configuration to follow the ferromagnet without irreversible switching. The energy difference resulting from intergranular coupling leads to an additional torque acting on the ferromagnet (F) that appears as a bias field resulting in a shifted hysteresis.

In order to explore this idea, we have performed a finite element micromagnetic calculation of a ferromagnet/antiferromagnet bilayer. Technical details of the calculation are given elsewhere,[15] but the essential feature is that a two-lattice approach was developed, in which the spin directions on a length scale of the exchange length are combined to a magnetization direction on one finite element. The stray field is taken into account using a hybrid finite element–boundary element method. The finite element calculation for antiferromagnet/ferromagnet structures results in the same spin-flop coupling as obtained by micromagnetic calculations on an atomistic length scale.[5] In the remainder of the present paper we discuss a simplified version of this model suitable for examining very large ensembles of grains. The results agree well with those of the finite element model, but highlight most clearly the crucial role of randomness in the antiferromagnet necessary to generate exchange bias. We also show that this intrinsic dependence on randomness naturally provides a mechanism for training effects.

Before discussing the model and results, note should be made of two recently proposed mechanisms. Morosov and Sigov[12] proposed a model in which exchange bias appears due to a magnetic configuration generated between steps at an uncompensated interface. The grain model discussed here involves the formation of narrow domain walls between grains, along the interface. Our mechanism involves lateral walls of a sort, but applies to compensated interfaces, free of geometrical imperfections.

The second mechanism is called the domain state model, and has been proposed by Nowak, Misra, and Usadel.[14] This model describes an exchange bias due to domain-wall pinning by random defects. A net moment caused by uncompensated spins provides coupling across the interface, and the authors found a bias shift for directions parallel to the antiferromagnetic anisotropy axis for spins in a single-crystal lattice. Our model assumes no defects except for grain boundaries, and coupling is due to spin flop at a perfect compensated interface. The antiferromagnetic film is not a single crystal but instead a collection of small crystallites with randomly oriented axes. In our model the energy associated with exchange bias is stored in AF domain walls. The

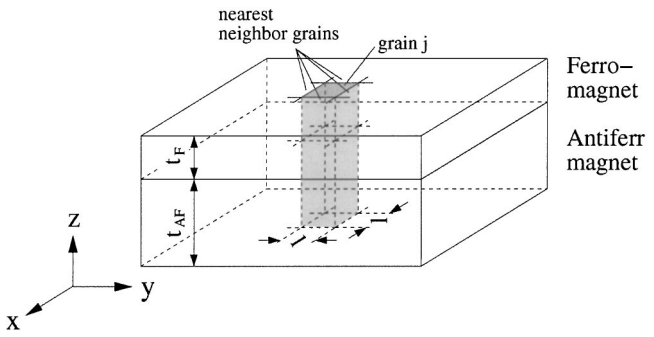

FIG. 2. Geometry of the interacting granular model. l is the grain diameter in the antiferromagnet and ferromagnet. t_{AF} and t_{F} are the thicknesses of the antiferromagnet and ferromagnet, respectively. One grain in the antiferromagnet and one in the ferromagnet are represented by the gray prism.

interface energy is merely to provide coupling to the antiferromagnetic domains, and otherwise plays no role in the formation of bias. In contrast, with the domain state model the interface energy is argued to play a dominant role in the formation of bias.

II. INTERACTING GRAIN MODEL

This model is described by a single grain energy composed of anisotropy, Zeeman, and intergrain exchange energy terms. We assume a polycrystalline antiferromagnetic film of thickness t_{AF} coupled to a polycrystalline ferromagnetic film of thickness t_{F}. For small grain size and low intergrain exchange coupling the magnetization within a grain remains nearly uniform. This means, for example, that a partial wall cannot form in a grain and there is a maximum thickness for which the model applies. We assume a compensated interface and therefore introduce a 90° coupling between the AF and F layers following suggestions by Stiles and McMichael[16] and as derived by Stamps.[17] The total energy per grain j is

$$E^j=\sum_{i=1}^{nN}\left[-J_{\mathrm{F}}S^2n_{\mathrm{F}}t_{\mathrm{F}}l\mathbf{u}_{\mathrm{F}}^j\mathbf{u}_{\mathrm{F}}^i-J_{\mathrm{AF}}S^2n_{\mathrm{AF}}t_{\mathrm{AF}}l\mathbf{u}_{\mathrm{AF}}^j\mathbf{u}_{\mathrm{AF}}^i\right]$$
$$-J_{\mathrm{AF\text{-}F}}S^2n_I(\mathbf{u}_{\mathrm{AF}}^j\mathbf{u}_{\mathrm{F}}^j)^2l^2-K_1(\mathbf{k}_{\mathrm{AF}}^j\mathbf{u}_{\mathrm{AF}}^j)^2t_{\mathrm{AF}}l^2$$
$$+(J_s^2/\mu_0)(\mathbf{k}_{\mathrm{F}}^j\mathbf{u}_{\mathrm{F}}^j)^2t_Fl^2-J_s\mathbf{H}\mathbf{u}_{\mathrm{F}}^jt_{\mathrm{F}}l^2. \qquad (1)$$

The sum over i is over the nearest-neighbor grains. S is the total spin quantum number, and l the grain diameter. J_{F} and J_{AF} denote the exchange integral across ferromagnetic grains and antiferromagnetic grains, respectively. $J_{\mathrm{AF\text{-}F}}$ describes the total effective exchange interaction at the compensated interface. The exchange energies depend on the number of spins per area at the interface, n_I, at the ferromagnetic grain boundary, n_{F}, and at the antiferromagnetic grain boundary, n_{AF}. The geometry used in defining Eq. (1) is shown in Fig. 2. $\mathbf{u}_{\mathrm{AF}}^j$ and $\mathbf{u}_{\mathrm{F}}^j$ denote the unit vectors of the spin direction in the grain j of the antiferromagnet and ferromagnet, respectively. The third term in Eq. (1) describes the 90° coupling associated with a canted spin-flop state formed at a compensated interface. The antiferromagnetic spins are not fully antiparallel near the interface. This canted state is strongly localized to the interface. In the bulk of the antiferromagnet the spins of the different sublattices are antiparallel for the typical fields applied in applications. This means that as long as the applied field is not larger than the antiferromagnetic exchange, as is the case in most experiments, magnetic surface and volume charges cancel in the antiferromagnet. Any remaining contributions to magnetostatic energy for individual magnetic sublattices in the antiferromagnet can be taken into account through the anisotropy constant K_1. Shape effects for the ferromagnetic film are approximated with the fifth term in Eq. (1) by assuming an in-plane anisotropy energy proportional to the square of the magnetization. In this term, k_{F} is a unit vector pointing perpendicular to the film plane. The antiferromagnet has uniaxial anisotropy of strength K_1 and the easy axis direction $\mathbf{k}_{\mathrm{AF}}$ is assigned randomly for every grain. Finally, we assume that an external static magnetic field $\mathbf{H}$ only acts on the ferromagnet. This energy is given by the sixth term in Eq. (1) where J_s is the magnitude of the spontaneous magnetization.

Hysteresis loop calculations are made by first initializing the system by simulating field cooling and then following the evolution of the magnetization with changing the applied magnetic field. An equilibrium configuration is found at each magnetic-field value. The equilibrium state is obtained by the numerical integration of the Landau-Lifshitz-Gilbert[18] (LLG) equation using effective fields determined from the energy in Eq. (1). The field acting on the antiferromagnet is found using

$$\mathbf{H}_{\mathrm{eff,AF}}^j=-\frac{1}{J_st_{\mathrm{AF}}l^2}\frac{\partial E_{\mathrm{tot}}}{\partial\mathbf{u}_{\mathrm{AF}}^j}, \qquad (2)$$

where $J_st_{\mathrm{AF}}l^2$ is the total sublattice moment of the antiferromagnetic component of grain j. A similar expression is used to calculate the effective field acting on the ferromagnet. We assume the system to be in equilibrium if the change of the magnetization, $d\mathbf{u}/dt$, is smaller than 10^{-4} on every node. A backward differentiation method[19] is used to integrate the LLG equation numerically.

III. BIAS FIELDS AND TRAINING

For the following, simulation parameters are chosen to approximate materials used in giant magnetoresistance read heads, such as IrMn. In the antiferromagnet, $K_1=1\times10^5$ J/m^3, $J_{\mathrm{AF}}=0.023$ meV. The antiferromagnetic layer consists of 60×60 rectangular grains with a basal plane area 10×10 nm^2. The grain structure in the ferromagnet is the same as in the antiferromagnet. The thickness of the ferromagnet is 10 nm in all cases. The intergrain interaction between ferromagnetic grains is $J_{\mathrm{F}}=0.45$ meV. The coupling between the ferromagnet and antiferromagnet is completely compensated, with the effective interface exchange, $J_{\mathrm{AF\text{-}F}}=-0.45$ meV.

Calculated hysteresis loops for an antiferromagnet thickness of 20 nm are shown in Fig. 3. To initialize the system, field cooling is simulated using a Metropolis Monte Carlo

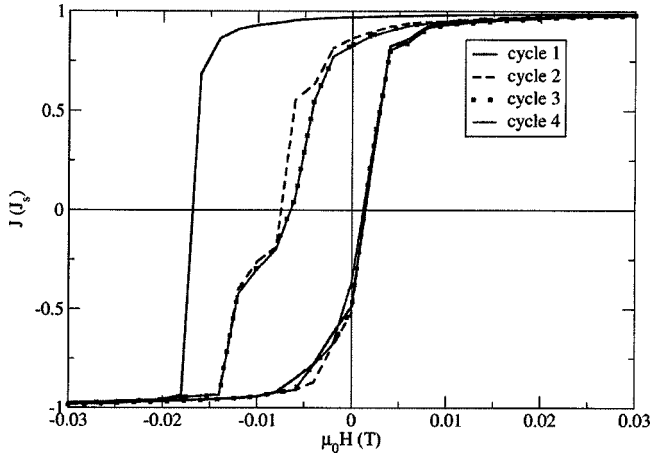

FIG. 3. Calculated hysteresis loops for a IrMn/Permalloy bilayer. The IrMn thickness and the grain size are 20 and 10 nm, respectively. The thickness of the ferromagnet is 10 nm. The interface is completely compensated. The bias field decreases with the number of hysteresis cycles.

algorithm. The ferromagnet direction is fixed, and the magnetization of the antiferromagnet is set randomly. Three different trial steps[20] are used to efficiently sample the phase space of spin configurations. Each Monte Carlo step begins by randomly choosing an antiferromagnetic grain and making the following three tests, each chosen according to a Metropolis Monte Carlo algorithm: A new magnetization direction is randomly chosen (i) within a cone of an angle of 3° such that the symmetry axis of the cone is parallel to the old magnetization direction, (ii) within any orientation on a sphere, and (iii) as a simple reversal. We start the cooling process at a temperature of $T=800$ K and decrease the temperature to $T=0$ in steps of $\Delta T=25$ K. At each temperature we scan the lattice 2000 times.

The initial field strength is $\mu_0 H=0.1$ T and is decreased in steps of $\mu_0 \Delta H=-0.002$ T. The field direction is parallel to the *y* axis. In order to investigate the training effect several hysteresis cycles are calculated. Cycle 1 of the loops in Fig. 3 is calculated starting from the field cooled state as the initial configuration and has a bias field of $\mu_0 H_b=7.7$ mT. The next cycle (cycle 2) shows a reduction of the bias field by about 65%.

Because the hysteresis loops are obtained at zero temperature there are no effects due to thermal fluctuations. Training appears only because the domain configuration in the antiferromagnet is strongly dependent on a history created by irreversible switching of antiferromagnets in the ensemble of grains. The ferromagnet orientation does not change during cooling. After cooling, the only equilibration process available to the antiferromagnet appears through changes in the state of the ferromagnet. Only a fraction of the antiferromagnet grains reverses during each cycle, but some grains do not. The relative magnitude of these two populations in a steady-state configuration is essentially a self-consistent solution that minimizes the total energy of the many-grain ensemble. It is not necessarily the lowest-energy solution and is sensitive to the initial conditions, size of the applied field step used, and applied field limits. In our simulations, a steady-state equilibrium appeared after about four cycles.

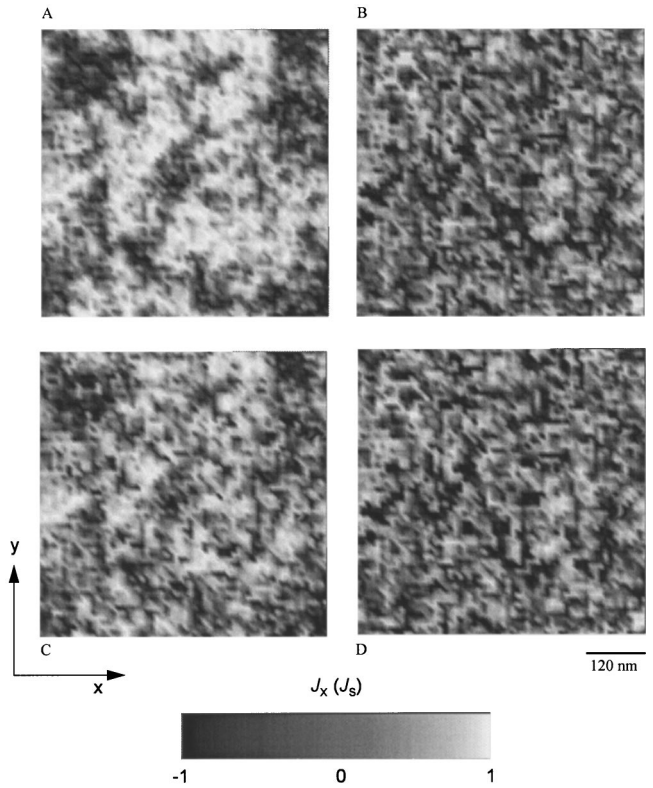

FIG. 4. Domains in the antiferromagnet. The *x* component of one antiferromagnet sublattice is indicated by a gray scale. The properties of the antiferromagnet are the same as those in Fig. 3. (a) State after field cooling. $\mu_0 H_{ext}=0.1$ T. (b) $\mu_0 H_{ext}=-0.1$ T. (c) Domain structure after the first hysteresis cycle. $\mu_0 H_{ext}=0.1$ T. (d) $\mu_0 H_{ext}=-0.1$ T.

The approach to a steady-state solution is illustrated in Fig. 4. In this figure, domain configurations at different points along the magnetization curve are shown after field cooling using gray scales to indicate the orientation of one antiferromagnet sublattice. The magnetization of one sublattice of the antiferromagnet parallel to the *x* axis is indicated by a gray scale (left=black;right=white). The external field in Fig. 4(a) is $\mu_0 H_{ext}=0.1$ T. Note the formation of large domains with diameters of several hundred nanometers. This is consistent with the thermal annealing and cooling at high field, which favors formation of uniform domains with a minimum of domain boundary walls.

The domain configuration in the antiferromagnet at $\mu_0 H_{ext}=-0.1$ T after the reversal of the ferromagnet is shown in Fig. 4(b). The large domains seen in Fig. 4(a) break up into a number of smaller domains. This represents a higher-energy configuration than in Fig. 4(a) because of the increase in energy involved in creating domain walls.

The domain configuration is shown in Fig. 4(c) for the system after it is brought back to the field $\mu_0 H_{ext}=0.1$ T as the first loop is completed. The domains are larger than in Fig. 4(b), corresponding to a lower total energy since the number of domain walls is reduced. Note, however, that a number of antiferromagnetic grains did not reverse back to their original orientation just after field cooling. Consequently the domains in the antiferromagnet are somewhat

smaller on average than in Fig. 4(a), and the total energy is also higher.

It is interesting that even though this is a zero-temperature process, the original field cooled configuration will never again appear as the field is cycled further. The reversed ferromagnet configuration for the second cycle $\mu_0 H_{\text{ext}} = -0.1$ T point is shown in Fig. 4(d). The steady-state configuration is not yet achieved and the high-energy state of Fig. 4(d) is different from that in the first cycle shown in Fig. 4(b). The origin of this athermal behavior is in the nature of the antiferromagnet ordering. As pointed out above, the antiferromagnet is affected not by the applied field directly, but instead through exchange coupling to the ferromagnet. During the demagnetization and magnetization branches of a cycle, the ferromagnet locally aligns in such a way as to minimize competing energies due to the applied field and exchange energies through coupling with the antiferromagnet. The random anisotropy axes of the antiferromagnet force the ferromagnet to adopt an equilibrium configuration that varies spatially. From the point of view of the antiferromagnet, the orientation of the ferromagnet varies spatially and creates a random field whose exact configuration depends on the applied field strength. In this way the antiferromagnet responds to a series of different spatially distributed random fields during a magnetization loop cycle.

The exchange bias hysteresis loop shift persists after cycling and is due to the fraction of grains that remain fixed during the magnetization process and intergranular exchange energy incurred with adjacent grains that reverse. An example is shown in Fig. 5 for two grains. Arrows in the antiferromagnet identify one sublattice only for simplicity. After field cooling the ferromagnet and this sublattice of the antiferromagnet are aligned, corresponding to a low-energy state. Upon reversal, the grain on the right (G_1) remains fixed, but the grain on the left (G_2) switches. G_1 did not switch because its axis is aligned with a component normal to the film plane. The easy axis in G_2 is parallel to the film plane that allows a 180° rotation of the antiferromagnet magnetization as the ferromagnet is reversed. Because of the antiparallel orientation of the spins in the reversed state this state has a larger intergranular exchange energy than the field cooled state.

The energy involved in forming pinned domain walls between antiferromagnetic grains is responsible for the exchange bias shift. After the steady state is reached, this energy can be recovered by untwisting the wall. The intergranular energy is plotted in Fig. 6 as a function of the applied field for several cycles. The minimum energy is always in the field cooling direction regardless of the cycle, and takes the smallest value directly after field cooling and before cycling. The total energy increases when the ferromagnet switches, as discussed above.

The complicated history dependence demonstrated during cycling is due to competition between ferromagnetic and antiferromagnetic components of the grains originating in interlayer and intergrain exchange interactions. These dependencies are illustrated in Fig. 7 where the bias field and coercivity are shown as a function of intergranular exchange. The coercivity is shown by triangles, and is measured as the zero magnetization width of the first hysteresis loop. The maximum coercivity occurs for small nonzero values of intergranular exchange and represents the low energy involved with irreversibly switching grains. The coercivity decreases almost linearly with increasing intergranular exchange as the energy cost of reversing grains increases.

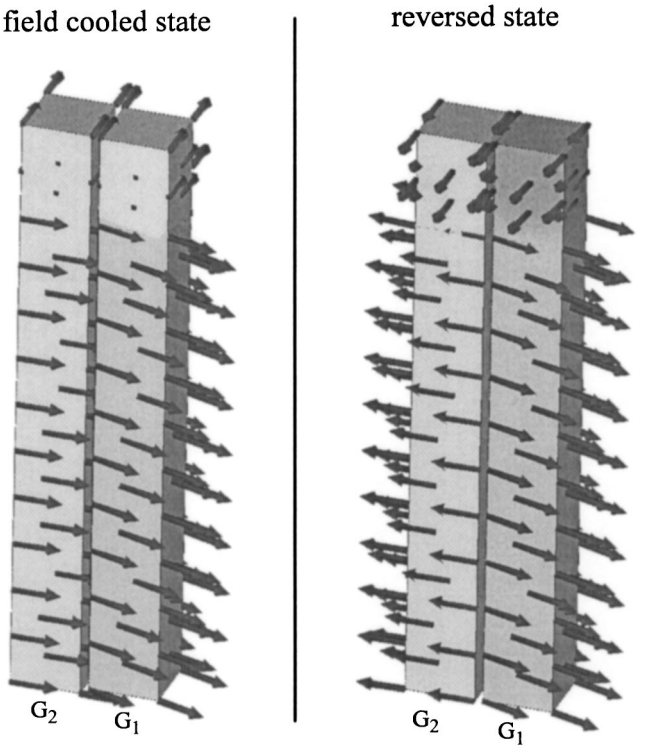

FIG. 5. Spin configuration of an granular AF/F bilayer after field cooling and after the reversal of the ferromagnet, respectively. The magnetization of one sublattice is shown in the antiferromagnet. The easy axis of G_1 is parallel to the AF/F interface. The angle between the easy axis of G_2 and the interface is 10°. After field cooling the magnetization of the two grains points almost parallel. After switching of the ferromagnet only G_2 reverses.

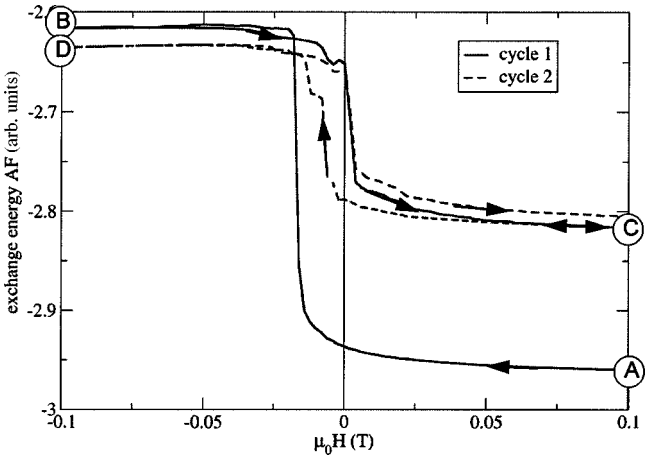

FIG. 6. Exchange energy in the AF as a function of the external field strength for the first and second hysteresis cycles. The states (A)–(D) are the same as those in Figs. 4(a)–4(d).

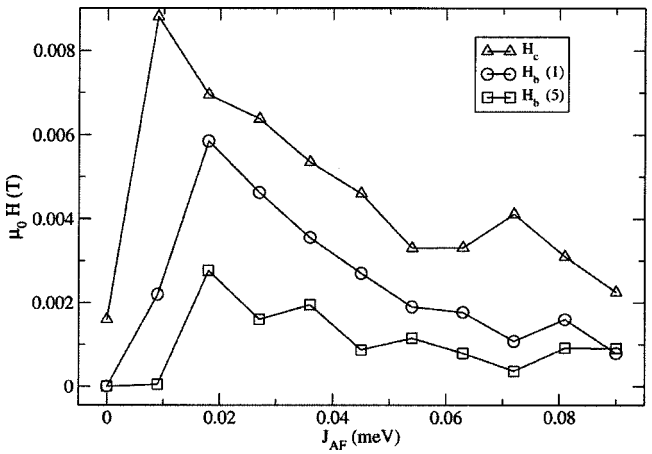

FIG. 7. Bias field of different hysteresis cycles and coercivity as a function of the intergranular exchange. H_b (1) and H_b (5) denote the exchange bias fields of the first and fifth hysteresis cycles, respectively. The difference between H_b (1) and H_b (5) shows the training effect. H_c is the coercive field of the first hysteresis cycle.

The bias field as a function of intergranular exchange for the first magnetization loop is indicated by circles in Fig. 7. The bias shift depends on intergranular exchange J_{AF} in a different manner from the coercivity because of the way in which the bias depends upon reversible changes in the antiferromagnetic order. Because of this, the first loop bias has a maximum for J_{AF} at about 0.02 meV, somewhat larger than the value corresponding to the maximum in coercivity. The bias shift is reduced for larger J_{AF} since it becomes energetically less favorable to create misalignment between neighboring grains.

The bias field as a function of J_{AF} is shown in Fig. 7 with squares for the fifth magnetization loop. A weak maximum appears again for J_{AF} at about 0.02 meV, but the overall magnitude of the bias is much reduced from that of the first loop. As mentioned above, this training effect is a consequence of the way in which the system approaches a low-energy steady-state configuration.

A quantity related to the intergrain exchange energy is the thickness of the antiferromagnetic film. The contact area between grains controls the intergranular exchange energy. The intergranular energy density therefore scales with film thickness. For this reason, the exchange terms in Eq. (1) depend on the thickness of the antiferromagnet. The antiferromagnet thickness is therefore an experimentally accessible parameter that affects directly the interaction between grains.

The bias field for different thicknesses of the antiferromagnet is shown in Fig. 8. The bias field was calculated for the tenth hysteresis cycle. Because the domain-wall energy in our model is proportional to the contact area between grains, the domain-wall energy increases with increasing antiferromagnet film thickness. The corresponding bias field also increases for small thicknesses. The bias field shows a maximum for a thickness of 22 nm as volume effects of the anisotropy begin to appear. For large thicknesses the high anisotropy energy hinders switching of the antiferromagnetic grains and results in a small bias field. The bias field therefore decreases for film thicknesses larger than 22 nm.

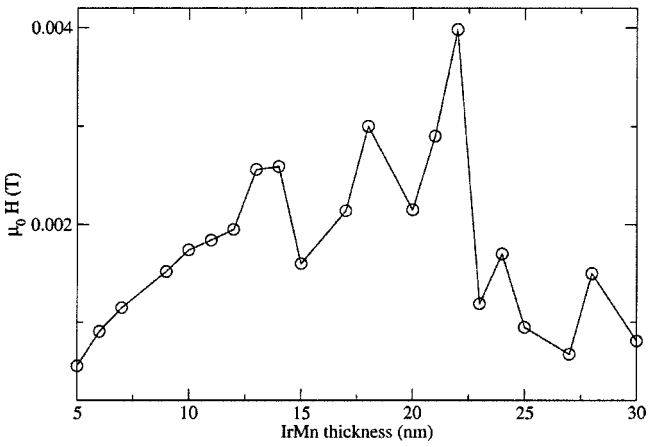

FIG. 8. Bias field as a function of the thickness of the antiferromagnetic IrMn layer. The bias field is calculated for the tenth hysteresis cycle.

The thickness dependence of the bias field of our model agrees well with experiments of van Driel *et al.*,[21] in which the thickness dependence of granular IrMn/Permalloy bilayers with random easy axes distribution in the AF was measured. Note that our model predicts a finite bias field for film thicknesses below the domain-wall thickness, in contrast to partial wall models of exchange bias.[6,11] van Driel *et al.*[21] compared the thickness dependence of the bias field of $\langle 111 \rangle$ textured films and films with random orientation of anisotropy axes in the IrMn layer. In the textured films the maximum of the bias field as a function of the AF thickness occurs at a lower thickness as compared to the film with random orientation. Similarly, the numerical simulations based on the interacting grain model show a shift of the maximum towards smaller thicknesses with increasing texture. For example, in a textured film with a standard deviation of the easy axis of 20° the maximum occurs at 16 nm as compared to 22 nm, which is the position of the maximum for the films with random orientation of anisotropy axes. Exchange bias and the training effect of textured films are discussed in the following section.

IV. ANTIFERROMAGNETIC FILMS WITH TEXTURE

The above results assumed a flat distribution of anisotropy axes over all possible orientation angles. This is not the best approximation of actual experimental samples where the structure of granular materials may show on average a preferred orientation for crystalline axes. For example, King *et al.*[22] concluded from *x*-ray-diffraction patterns taken on NiFe/IrMn bilayers that the granular IrMn layer is textured with the $\langle 111 \rangle$ direction of the grains perpendicular to the interface.

In terms of magnetic anisotropies, such texturing corresponds to an average angle between the easy axis and the interface normal $\overline{\theta} = 54.74°$. In order to describe texture in our model, we have calculated bias shifts and coercivities with an angular distribution of anisotropy easy axes orientations. A Gaussian distribution of angles θ measured between the film normal and the easy axis is assumed:

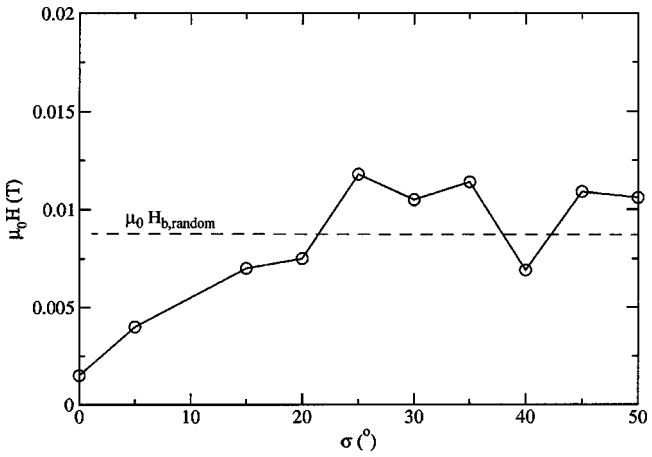

FIG. 9. Bias field shifts determined from the first hysteresis loop after field cooling are shown as a function of distribution width σ. The dotted line represents the bias field for a complete random distribution of the easy axes in the AF grains.

$$P(\theta)=\frac{1}{\sqrt{2\pi}\sigma}e^{-(1/2)(\theta-\bar{\theta})^2/\sigma^2}\sin(\theta). \tag{3}$$

The width of the distribution is given by the parameter σ.

Bias fields determined from the first magnetization loop after field cooling are shown in Fig. 9 as a function of distribution width σ. The following material parameters were used: $J_F=0.23$, $J_{AF}=0.023$, and $J_{AF\text{-}F}=-0.45$ meV, and $t_{AF}=20$ and $t_F=10$ nm. The average angle is assumed to be $\bar{\theta}=54.74°$. The bias shift exhibits a weak maximum for σ between 30° and 40° and remains near a constant value of 0.01 T for σ greater than 45°.

The axes distribution has the largest effect on the bias field only when the spread in angles is small. In other words, only the fraction of grains with relatively well-aligned axes parallel to the interface contribute to bias shifts. This means, for example, that bias fields for uniformly random axes distributions will in general be less than bias fields for textured samples with sufficient large σ. This is, in fact, what we found upon comparing bias shifts for systems with texture, as shown in Fig. 9, to systems with axes distributed randomly but uniformly on a sphere.

It is relevant to note that there is little dependence of the bias shift on the shape of the distribution for such a narrow angular range. In consequence, the bias field shift calculated using a uniform distribution of axes restricted to a range of magnitude σ is little different from that calculated using a Gaussian distribution of width σ.

In contrast to the bias field, the coercive field is not as strongly affected by the width of the distribution. Coercivity exists because of irreversible rotations of the ferromagnet, to which irreversible processes in the antiferromagnet also contribute. It is interesting to examine the dependence of the numbers of grains switched in the antiferromagnet to bias and coercive fields for different anisotropy axis distribution widths. A summary is given in Table I in which bias and coercive fields for different σ are listed together with the percentage of antiferromagnet grains switched during the magnetization loop.

TABLE I. The bias field ($\mu_0 H_b$) and the coercive field ($\mu_0 H_c$) of the first hysteresis cycle, the percentage of irreversible switched grains in the AF, and the percentage of formed domain walls in the AF after reversal of the F are given for different values of the standard deviation of the texture.

σ (°)	0	5	15	25	35	45	50
$\mu_0 H_b$ (mT)	1.5	4.0	7.1	11.8	11.4	10.9	10.6
$\mu_0 H_c$ (mT)	14.5	16.2	22.0	20.8	20.4	16.0	13.7
Switched grains (%)	2.9	4.0	11.1	17.8	20.2	20.1	17.9
Wall formation (%)	5.0	6.7	14.8	20.8	23.2	23.7	22.9

The number of switched grains is determined at the zero-field points of the first magnetization loop made after field cooling. Switching for canted antiferromagnet sublattice magnetizations is defined in terms of the "**I**" introduced in Fig. 1. Switching is said to occur when the component of **I** along the anisotropy direction of a grain changes sign.

There is a clear correlation between the width of the distribution σ, percentage of switched grains, and the bias shift. Less clear is the relation between σ, the percentage of switched grains, and the coercive field. A key point in the bias mechanism proposed here is that switching of grains in the antiferromagnet contributes to both bias field and coercivity observed through the ferromagnet. However the bias shift depends exclusively on the formation of domain walls between grains. These walls do not form unless some, but not all, antiferromagnets switch. Example percentages of walls formed are listed in Table I for different axes distribution widths. The percentages are measured as the number of misaligned neighboring grains relative to the total number of possible misalignments. Misalignment is defined for a pair if one grain has switched but other has not.

V. SUMMARY AND CONCLUSIONS

In this paper a type of partial wall model of exchange bias has been presented in which the partial walls are formed along the interface in a granular antiferromagnetic film. The mechanism is similar to that proposed by Malozemoff, except that our mechanism describes both coercivity and bias through walls localized between grains and applies directly to systems with interfaces compensated at an atomic scale. We have shown that a relatively simple model can be used to quantify bias and coercivity fields with predicted magnitudes on an order comparable to those observed experimentally. The main conclusion is that the important mechanism governing bias in the random granular antiferromagnet is the intergrain exchange coupling. The proposed mechanism contributes to exchange bias whenever the domain structure in the antiferromagnet changes during the reversal of the ferromagnet. A key point is that irreversible switching in the antiferromagnet is therefore necessary for bias field formation. Coercivity observed through the ferromagnet may be en-

hanced by irreversible switching in the antiferromagnet, but ferromagnetic coercivity can also exist independently.

The mechanism for bias proposed here applies only for grains that are smaller than an antiferromagnet wall width. One consequence is that our results are strictly valid only for intergrain exchange coupling that is weak compared to the intergrain exchange so that a partial wall cannot form within a grain. Furthermore, the weak intergrain exchange coupling is important for the irreversible switching of some grains, which is a necessary component of our model. In the limit of vanishing intergrain exchange, the finite element calculations show that it is not possible to reverse grains in a thin antiferromagnetic film if the easy axis is not parallel to the interface.

The results of the granular partial wall model are in good agreement with calculations made using a finite element solution which allows for nonuniform magnetization within grains. The only additional features revealed by finite element calculations are additional dependencies on grain height and intergrain coupling in the limit of strong intergranular exchange. The grain height dependence is in fact very important, since the mechanism we propose only works for thin antiferromagnetic films. Using finite element models for thick antiferromagnetic films, we find that the bias has a maximum at a small antiferromagnetic film thickness, and decreases to zero for very thick antiferromagnetic grains. The reason for this is that the anisotropy energy contained in the grains, which is proportional to the grain volume, becomes larger than the intergranular exchange energy.

ACKNOWLEDGMENTS

This work was supported by the Austrian Science Fund Grant No. Y-132 PHY. R.L.S. and J.K. also acknowledge support from the Australian Research Council.

*Author to whom correspondence should be addressed. FAX: +43-1-58801-13798. Email address: suess@magnet.atp.tuwien.ac.at

[1] W. H. Meiklejohn and C. P. Bean, Phys. Rev. **102**, 1413 (1956).
[2] J. Nogués and K. Schuller, J. Magn. Magn. Mater. **192**, 203 (1999).
[3] T. Ambrose, R. L. Sommer, and C. L. Chien, Phys. Rev. B **56**, 83 (1997).
[4] V. I. Nikitenko, V. S. Gornakov, L. M. Dedukh, Yu. P. Kabanov, and A. F. Khapikov, Phys. Rev. B **57**, 8111 (1998).
[5] N. C. Koon, Phys. Rev. Lett. **78**, 4865 (1997).
[6] T. C. Schulthess and W. H. Butler, Phys. Rev. Lett. **81**, 4516 (1998).
[7] A. E. Berkowitz and J. H. Greiner, J. Appl. Phys. **36**, 3330 (1965).
[8] L. Neel, Ann. Phys. (N.Y.) **2**, 61 (1967).
[9] H. Fujiwara, K. Zhang, T. Kai, and T. Zhao, J. Magn. Magn. Mater. **235**, 319 (2001).
[10] A. P. Malozemoff, J. Appl. Phys. **63**, 3874 (1988).
[11] D. Mauri, H. C. Siegmann, P. S. Bagus, and E. Kay, J. Appl. Phys. **62**, 3047 (1987).
[12] U. Nowak, A. Misra, and K. D. Usadel, J. Appl. Phys. **89**, 7269 (2001).
[13] A. I. Morosov and A. S. Sigov, J. Magn. Magn. Mater. **242–245**, 1012 (2002).
[14] T. C. Schulthess and W. H. Butler, J. Appl. Phys. **85**, 5510 (1999).
[15] D. Suess, T. Schrefl, W. Scholz, J. V. Kim, R. L. Stamps, and J. Fidler, IEEE Trans. Magn. **38**, 2398 (2002).
[16] M. D. Stiles and R. D. McMichael, Phys. Rev. B **59**, 3722 (1999).
[17] R. L. Stamps, J. Phys. D **33**, 247 (2000).
[18] J. C. Mallinson, IEEE Trans. Magn. **30**, 62 (1987).
[19] A. C. Hindmarsh and L. R. Petzold, Comput. Phys. **9**, 148 (1995).
[20] D. Hinzke and U. Nowak, Phys. Rev. B **58**, 265 (1998).
[21] J. van Driel, F. R. de Boer, K.-M. H. Lenssen, and R. Coehoorn, J. Appl. Phys. **88**, 975 (2000).
[22] P. King, I. N. Chapman, M. F. Gillies, and J. C. S. Kools, J. Phys. D **34**, 528 (2001).